

1 Unique protein features of SARS-CoV-2 relative to other Sarbecoviruses

2

3

4 Matthew Cotten^{1,2}, David L. Robertson², My V.T. Phan¹

5

6 Affiliations

7 1. MRC/UVRI & LSHTM Uganda Research Unit, Entebbe, Uganda

8 2. MRC-University of Glasgow Centre for Virus Research, Glasgow, UK

9 Correspondence: Matthew Cotten (Matthew.Cotten@lshtm.ac.uk)

10 **Keywords:** SARS-CoV-2, proteome changes, *Sarbecovirus* evolution, spike protein changes

11

12 Abstract

13 Defining the unique properties of SARS-CoV-2 protein sequences, has potential to explain the
14 range of Coronavirus Disease 2019 (COVID-19) severity. To achieve this we compared proteins
15 encoded by all Sarbecoviruses using profile Hidden Markov Model similarities to identify protein
16 features unique to SARS-CoV-2. Consistent with previous reports, a small set of bat and pangolin-
17 derived Sarbecoviruses show the greatest similarity to SARS-CoV-2 but unlikely to be the direct source
18 of SARS-CoV-2. Three proteins (nsp3, spike and orf9) showed differing regions between the bat
19 Sarbecoviruses and SARS-CoV-2 and indicate virus protein features that might have evolved to support
20 human infection and/or transmission. Spike analysis identified all regions of the protein that have
21 tolerated change and revealed that the current SARS-CoV-2 variants of concern (VOCs) have sampled
22 only a fraction (~31%) of the possible spike domain changes which have occurred historically in
23 Sarbecovirus evolution. This result emphasises the evolvability of these coronaviruses and potential for
24 further change in virus replication and transmission properties over the coming years.

25

26 Introduction

27 Since the first report of Coronavirus Disease 2019 (COVID-19) caused by SARS-CoV-2 in
28 December 2019 in Wuhan city, China (Li et al. 2020)(Yang et al. 2020) and the World Health
29 Organisation declaring COVID-19 a global pandemic in March 2020, the disease has proceeded to
30 affect every part of the world. The SARS-CoV-2 virus belongs to the *Coronaviridae* family of enveloped
31 positive-sense single-stranded RNA viruses, *Betacoronavirus* genus, *Sarbecovirus* subgenus. Other
32 Sarbecoviruses include SARS-CoV (the coronavirus causing the SARS outbreak in 2002-2004) and a
33 large number of SARS-like bat viruses. The genomes of Sarbecoviruses are 30kb in length, encoding
34 >14 open reading frames (ORFs). Among the structural proteins, the spike protein plays a crucial role
35 in virus host-cell tropism, host range, cell entry and infectivity, and is considered the main protein target
36 for protective immune responses. Other virus ORFs encode structural and accessory proteins, many of
37 which modulate important host responses to infection.

38 Investigation of the evolutionary history of SARS-CoV-2 shows a clear link to Sarbecoviruses
39 circulating in horseshoe bats although no direct animal precursor for SARS-CoV-2 has been identified
40 (Andersen et al. 2020) (Boni et al. 2020) (Zhang et al. 2020) (H. Zhou et al. 2020) (Lam et al. 2020).

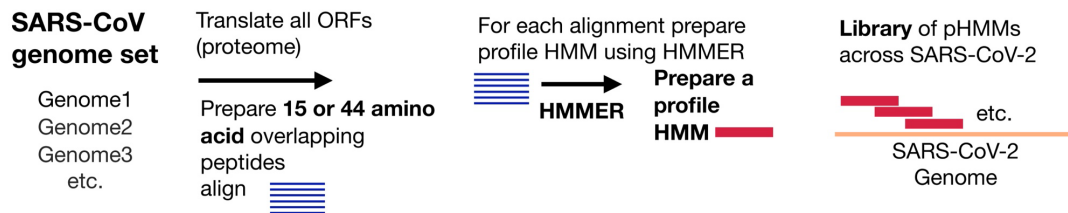
41 We sought to identify unique peptide regions of SARS-CoV-2 compared to all available *Sarbecoviruses*
42 to determine viral features that might be unique to SARS-CoV-2 and that might have allowed the virus to
43 infect, replicate and transmit efficiently in humans. Such a comparative analysis of viral proteins might
44 provide insights into the origin of the virus and identify the conditions that led to the zoonosis to humans,
45 efficient spread without the need for much, if any, adaptation (MacLean et al. 2021), as well as providing
46 leads for drug and immune targets for effective treatments.

47

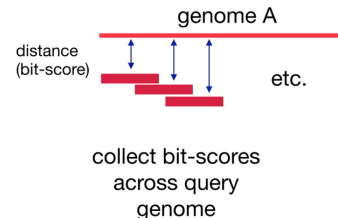
48 Results and Discussion

49 **Protein domains and profile hidden Markov models.** We have explored the genomes across
50 the *Sarbecovirus* subgenus using profile hidden Markov models (pHMMs). pHMMs can provide a
51 detailed statistical description of an amino acid sequence and can be used to detect related domains
52 found and to document their differences from a reference domain (Eddy 1998) (Eddy 1996). Efficient
53 tools for preparing and comparing pHMMs are available in the HMMER-3 package (Eddy 2011). This
54 approach is particularly useful for comparing large or evolutionary divergent genomes. We have
55 recently used these methods to identify and classify diverse coronaviruses in the *Coronaviridae* family
56 (Phan et al. 2018) and to explore large and unwieldy genomes such as those from the African Swine
57 Fever Virus (Masembe et al. 2020). Here pHMMs were used to explore the relationship between SARS-
58 CoV-2 and the other known *Sarbecoviruses* to gain understanding of their evolutionary history and to
59 identify regions of encoded viral proteins that are static to change or are altered across the
60 *Sarbecoviruses*.

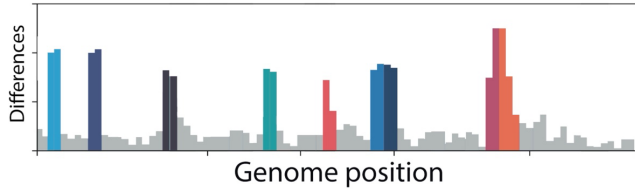
a. Prepare Agnostic Domains from a small set of early SARS-CoV-2 genomes



b. Use library to query related Sarbecovirus genomes



c. Identify protein domains (15 or 44 amino acids) that show differences from early SARS-CoV-2



61

62 **Figure 1. Analysis scheme.** (a) Profile Hidden Markov Model (pHMM) domains were generated from
63 a set of 35 early (Pango) lineage B SARS-CoV-2 genome sequences. All open reading frames
64 were translated and then sliced into either 44 amino acid peptides with a step size of 22 amino acids
65 or 15 amino acid peptides with a step size of 8 amino acid. The peptides were clustered using Uclust
66 (Edgar 2010), aligned with MAFFT (Katoh and Standley 2013) and then each alignment was built into
67 a pHMM using HMMER-3 (Eddy 2011). (b) The set of pHMMs were used to query *Sarbecovirus*
68 genome sequences, bit scores were collected as a measure of similarity between each pHMM and
69 the query sequence. (b) Bit-scores were gathered and analyzed to detect regions that differ between
70 early SARS-CoV-2 genomes and query genomes.

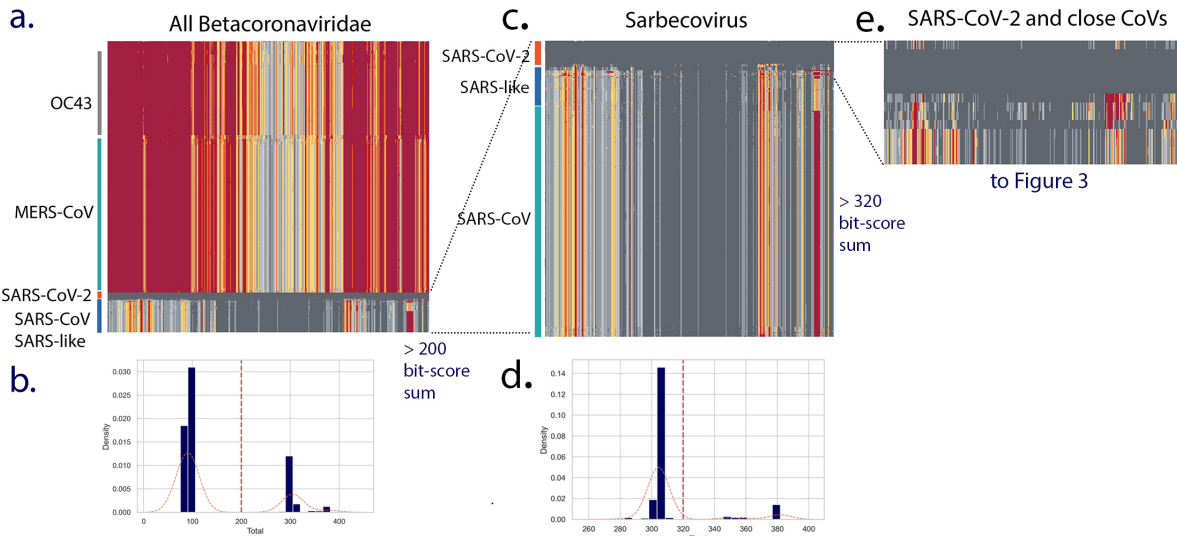
71

72

73 **Genome scans using custom pHMM domains.** First, some background on the strategy used
74 here. We sought to define the distance of any query virus genome from the early SARS-CoV-2 genome
75 that first began to infect humans in December 2019. To give two levels of resolution, we generated
76 overlapping 44 or 15 amino acid (aa) peptides from all early lineage B SARS-CoV-2 encoded proteins
77 then prepared pHMMs using HMMER-3 (see Figure 1a). The resulting libraries of pHMMs were then
78 used to survey domain diversity across query coronaviruses relative to the initial 2019 SARS-CoV-2.
79 For each pHMM match to a related sequence, a bit-score is generated which provides a metric for how
80 close the query sequence is to the pHMM (Figure 1b). These bit-scores, when collected across an
81 entire viral genome, can provide a sensitive description of similarities and difference between a query
82 genome and the reference genome (Figure 1c). For additional background on the method,
83 Supplementary Figure 1 demonstrates the the sensitivity of pHMMs to detect and distinguish single
84 amino acid substitutions and Supplementary Figure 2 demonstrates the use of pHMMs to identify single
85 amino acid substitution in a crucial region of the SARS-CoV-2 spike protein.

86 An initial triage was performed using all available Betacoronavirus genomes from GenBank. All
87 full genomes with the taxon id 694002 were retrieved, genomes with gaps were removed to yield a set
88 of 1480 Betacoronavirus genomes. SARS-CoV-2 genomes were initially excluded from the retrieval
89 and then a set of 27 early lineage B genomes were added as a reference. An additional 5 recently
90 reported bat CoV genomes not yet in GenBank (see Supplemental Table 1) were also added. The 44
91 aa pHMM library was used to query the Betacoronavirus set. For each genome, the bit-score each of
92 384 pHMMs from early lineage B SARS-CoV-2 sequences was collected and hierarchical clustering
93 based on the normalized domain bits-scores was performed (Figure 2a). Scores colored with dark to
94 light grey indicating domains identical or close to the corresponding domain from early lineage B SARS-
95 CoV-2 and yellow to orange to red indicating increasing distance. Within the Betacoronavirus set the
96 genomes clustered by their taxonomic group and clusters of OC43, MERS-CoV and SARS-CoV and
97 SARS-CoV-2 were observed. The central region of the *Sarbecovirus* genome is conserved across the
98 genome set with all domains marked as dark or light grey in the Figure 2a This is not unexpected as
99 this central region encodes the viral polymerase, other enzymes and non-surface exposed structural
100 proteins of the virus, which are functionally constrained and less likely to allow change than other
101 regions of the virus. In contrast, the domains displayed in yellow, orange and red in Figure 2a indicated
102 more increasingly divergent regions between early SARS-CoV-2 and the query *Sarbecovirus* genomes
103 (much lower normalized bit scores).

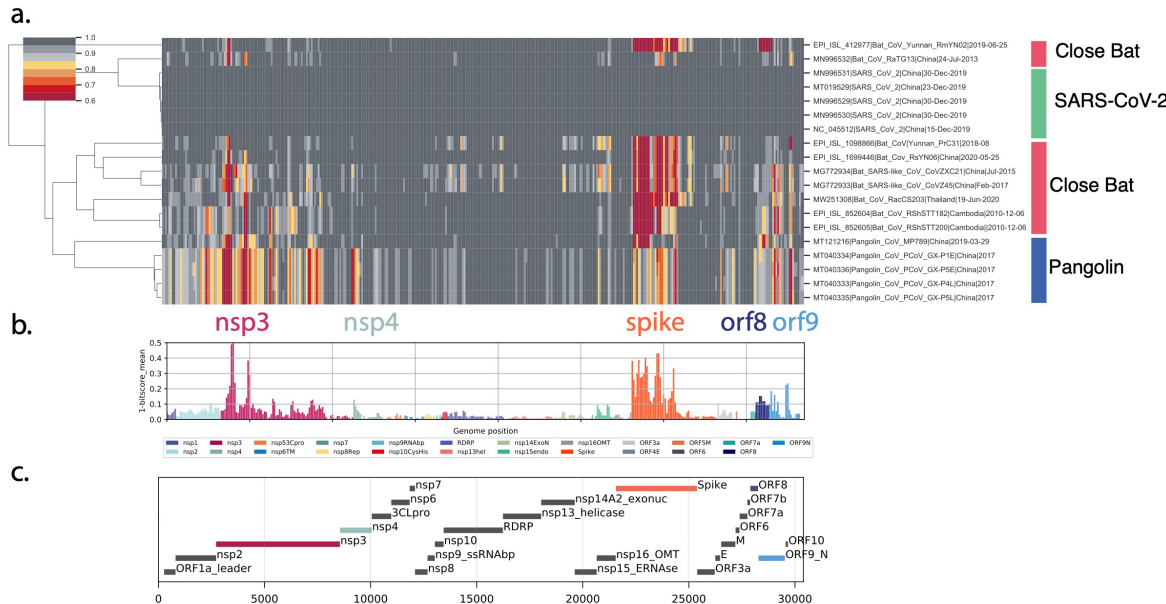
104 The sum of the entire set of bit-scores for a genome was then used to calculate a distance from
105 the early SARS-CoV-2 genome. A histogram of these bit-scores sums show several peaks (Figure 2b)
106 with majority of the Betacoronavirus genomes (mostly OC43 and MERS-CoV) clustering around 100
107 units and a subset of virus genomes with bit-scores >200 units. This >200 set included the SARS-CoV-
108 2, SARS-like CoVs from bats and all the SARS-CoV genomes (Figure 2c). A second triage retained a
109 set of close genomes all with bit-score sums >320 (Figure 2e) that was used more detailed analysis.
110 For simplicity, the 27 early B SARS-CoV-2 genomes in the set (which were nearly identical) were
111 reduced to 5 resulting in a 19 genomes in the close set: 14 bat/pangolin CoV and 5 SARS-CoV-2 (Figure
112 2e).



113

114 **Figure 2 Triage of Betacoronaviruses.** All Betacoronavirus genomes (excluding SARS-CoV-2) were
115 retrieved from GenBank using the query ((txid694002[Organism] AND 24000[SLEN]:40000[SLEN] NOT
116 patent)) NOT txid2697049[Organism]) generating a set of 1581 genomes that were screened to remove
117 genomes with gaps to yield a set of 1480 genomes. A small set of 27 early lineage B SARS-CoV-2
118 genomes from December 2019/January 2020 were added as markers. A library of 44 amino acid
119 pHMMs prepared from early B SARS-CoV-2 genomes was used and the bit-scores for each pHMM
120 were gathered and used to cluster the genomes (a) with each domain score indicated by color (dark
121 grey = 1 = very similar to SARS-CoV-2 to red = low = distant from SARS-CoV-2). The total bit-scores
122 sum for each genome was calculated (see histograms of all total bitscore sums (b)). A total bitscore
123 sum of 200 was used to select for the CoV genomes most similar to SARS-CoV-2. The clustering of
124 this subset of CoV genomes (c) included the SARS-CoV-2 genomes, a large number of SARS-CoV
125 genomes and a smaller number of SARS-like CoVs. A cut off of 320 for total bit-scores sum (d) was
126 used to identify the closest CoV genomes which were then used for the subsequent analyses reported
127 in Figures 3, 4 and 5.
128

129 We next focused on the bat Sarbecoviruses with closest similarity to SARS-CoV-2 in at least
130 part of their genomes due to recombinant histories (see Supplementary Table 1 for genome details and
131 references). The clustermap and variance analysis (Figure 3a) showed higher similarity across most of
132 the genome (dark grey sectors) with three proteins (nsp3, spike and orf9) displaying reduced bit-scores
133 compared to SARS-CoV-2 (Figure 3a, yellow, red domains). These differing regions between the bat
134 Sarbecoviruses and SARS-CoV-2 indicate virus protein features that might have evolved to support
135 human infection and/or transmission. The spike differences are explored in detail below however it may
136 be important to consider nsp3, ORF9 (and perhaps nsp4 and ORF8) in future analyses.



137

138 **Figure 3. Proteome differences in SARS-CoV-2 versus close bat Sarbecoviruses.** All forward open
 139 reading frames from the 35 early lineage B SARS-CoV-2 genomes were translated, and processed into
 140 44 aa peptides (with 22 aa overlap), clustered at 0.65 identity using Uclust (11), aligned with MAAFT
 141 (12) and converted into pHMMs using HMMER-3 (Eddy 2011). The presence of these domains was
 142 sought in a set of *Sarbecovirus* genomes plus the SARS-CoV-2 genomes. These were then clustered
 143 using hierarchical clustering based on the normalized domain bit-scores (e.g. the similarity of the
 144 identified query domain to the reference lineage B SARS-CoV-2 domain). Each row represents a
 145 genome, each column represents a domain. Domains are displayed in their order across the SARS-
 146 CoV-2 genome, Red = low normalized domain bit-score (lower similarity to lineage B SARS-CoV-2),
 147 i.e., higher distance from lineage B SARS-CoV-2, darkest grey = normalized domain bit-score = 1, i.e.,
 148 highly similar to lineage B SARS-CoV-2. Groups of coronaviruses are indicated to the right of the figure.
 149 **(a)** Domain differences across the *Sarbecovirus* subgenus. **(b)** For each domain the mean bit-score
 150 was calculated across the entire set of *Sarbecovirus genomes* and the value 1-mean bit-score was
 151 plotted for each domain. Domains are coloured by the proteins from which they were derived with the
 152 colour code indicated below the figure. **(c)** Schematic of open reading frames or protein products of
 153 SARS-CoV-2.

154

155 **Spike changes with 15 amino acid domains.** Using the same strategy described in Figure 3,
 156 we performed a triage of the Betacoronaviruses with 15 amino acid pHMMs prepared from early lineage
 157 B spike protein (Figure 4) and selected for CoV genomes encoding close Spike proteins. The high bit-
 158 score spike set largely overlapped with the high bit-score full genome set suggesting that spike is a
 159 good surrogate for full genome homology.

160 Key features of the spike protein are outlined in Figure 4c. The analysis revealed regions of
 161 spike that historically have tolerated change. In general the S1 subunit of spike (the amino-terminal
 162 half of the protein) displayed a large amount of diversity with most of the low score domains (more
 163 distant from SARS-CoV-2, marked in red) concentrated here (Figure 4a). This is consistent with the
 164 surface exposure of S1 on the virion and with protein changes driven by pressure to avoid immune
 165 responses. The central ACE2 receptor binding region (Figure 4c) was very different between the close
 166 Sarbecoviruses and SARS-CoV-2. The furin cleavage site at the junction between the S1 and S2
 167 domains (Figure 4c) is also a region showing a lot of diversity across the *Sarbecovirus* spikes (Figure
 168 4a) and appears completely unique to SARS-CoV-2. This has been discussed in detail (Hoffmann et
 169 al. 2020) and is also a site of frequent change in the current SARS-CoV-2 Variant of Concern (VOC)
 170 spike sequences with Q677, P681 and T717 flanking the furin site showing changes (Figure 4c).

171 The domains that where amino acid changes have appeared in VOC spike proteins are marked
 172 in color (Figure 4b) and largely appear in domains with high variation (Figure 4b, 1-mean bit-score >
 173 0.3) suggesting that Sarbecoviruses have made changes in these regions in previous evolutionary
 174 periods and are continuing to change in SARS-CoV-2 evolution. Of the 88 spike domains showing high
 175 variation in Sarbecoviruses (1 - mean bit-scores ≥ 0.3 units), only 27 of the domains (31%) have
 176 accumulated substitutions or deletions. This indicates a very large potential in the SARS-CoV-2 spike
 177 protein for tolerating future change. Important regions that have shown high levels of historical change
 178 are the NTD, the RBD and the furin cleavage site and flanking regions.

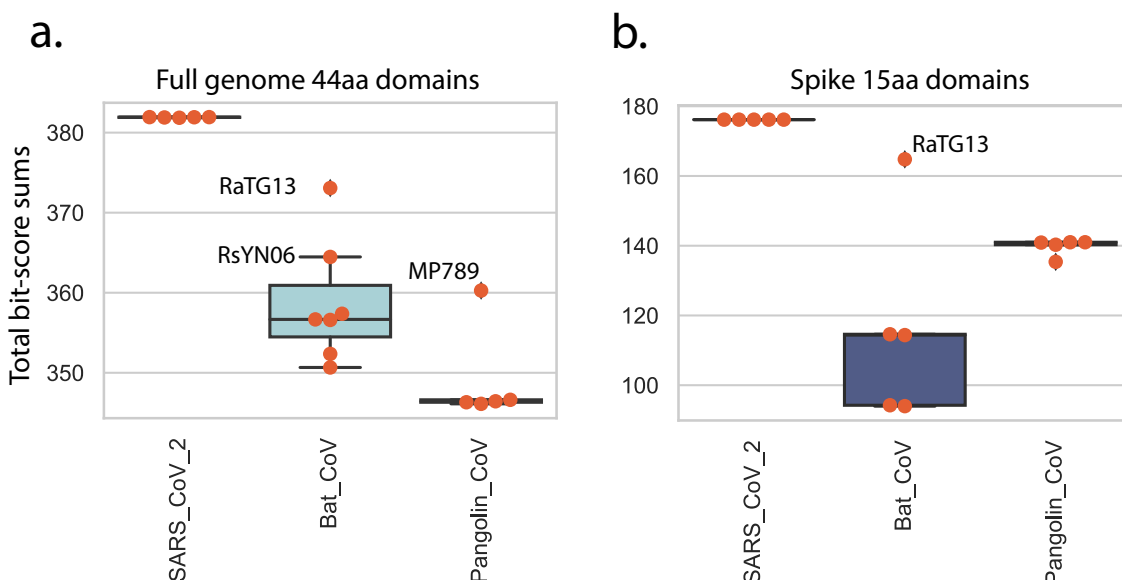


179
 180 **Figure 4. Spike differences in SARS-CoV-2 versus close bat Sarbecoviruses.** All forward spike
 181 open reading frames from the 35 early lineage B SARS-CoV-2 genomes were translated, and
 182 processed into 15 aa peptides (with 8 aa overlap) and processed into an pHMM library as described in
 183 Figure 2. **(a)** Shows a hierarchical clustering of 15 amino acid domain bit-scores. **(b)** Shows the 1-mean
 184 of each domain bit-scores across the genome set, domain values, individual domains that span known
 185 amino acid changes in the 6 VOC and VOIs (B.1.1.7, B.1.351, B.1.525, P.1, B.1.617.2 and A.23.1) are
 186 colored (see key below panel B). **(c)** The locations of important spike protein features are indicated.
 187 NTD: N-terminal domain, RBD: receptor-binding domain, S1: spike 1, S2: Spike 2, TM: transmembrane
 188 domain, HR1: helical repeat 1, HR2: helical repeat 2, NTD super: N-terminal domain supersite.
 189

190 **Global proteome similarities.** As described in Figure 2, a measure of the total protein distance
 191 between the SARS-CoV-2 and any query Sarbecovirus can be obtained by summing the normalized
 192 bit-scores (SNBS) across the entire query proteome. We examined SNBSs grouped by virus host for
 193 the 44 amino acid total genome analysis and the 15 amino acid spike gene analysis. The potential role
 194 of pangolins as an amplifying intermediate host of SARS-CoV-2 is important to document securely, to
 195 guide efforts to prevent or prepare for future zoonotic events. A small number of Sarbecoviruses have
 196 been identified in samples from trafficked pangolins in China (Liu et al. 2019) (Lam et al. 2020) (Xiao et
 197 al. 2020), yet there is no direct evidence that pangolins host the virus in their natural environment. It is

198 thus likely these pangolins identified in China were infected by viruses encountered after transport to
199 China, consistent with reports of disease in these animals. Five CoV sequences from pangolins were
200 included in this analysis (Supplementary Table 1), including four generated by Lam *et al.* (Lam *et al.*
2020) after sequencing the original samples described by Liu *et al.* (Liu *et al.* 2019); a 5th genome
202 (MP789) was deposited by Liu *et al.*.

203 The bat coronavirus genome RaTG13 (GenBank MN996532.1) was identified as closely related
204 to the SARS-CoV-2 lineage (P. Zhou *et al.* 2020) and supports a bat coronavirus being the zoonotic
205 source of the epidemic, although despite the close genetic distance it is too far in time (decades) for
206 RaTG13 itself to be a direct source of the pandemic SARS-CoV-2 virus (Boni *et al.* 2020). The next
207 closest bat coronavirus RsYN06, shows some regions of even close identity to SARS-CoV-2 than
208 RaTG13 (H. Zhou *et al.* 2020) (Figure 4a) due its possible recombinant nature. A single pangolin derived
209 SARS-CoV-2 (MP789) showed an SNBS value that was also elevated but not as high as the RaTG13
210 (Figure 5a), the 15 aa spike analysis showed similar patterns except that only the RaTG13 spike
211 displayed the high similarity to SARS-CoV-2 (Figure 5b).
212



213
214
215 **Figure 5.** Total domain distances between virus groups. Normalized bit-score sums (NBSS) grouped
216 into SARS-CoV-2 and Sarbecoviruses from pangolin, bat, for all domains for each genome were
217 summed. The boxplot shows individual values marked in orange, median values indicated by horizontal
218 black lines, 1st interquartile ranges marked with a box. The identities of several high scoring bat and
219 pangolin genomes are indicated. **(A)** NBSS for 44 aa domains across the entire coronavirus genome.
220 **(B)** NBSS for 15 aa domains across the spike protein.

221
222

223 **Conclusions**

224 What is special about SARS-CoV-2? Spike changes in SARS-CoV-2 compared to the close set
225 of Sarbecovirus genomes indicate that the immediate zoonotic source of SARS-CoV-2 is yet to be
226 identified due to the unique nature of the SARS-CoV-2 genome. The more detailed analysis of spike
227 regions in SARS-CoV-2 genomes (Figure 3) revealed the extent of the changes that have occurred
228 across the Sarbecoviruses. Combined with the current VOC spike changes (from lineages B.1.1.7,
229 B.1.351, B.1.525, P.1, B.1.617.2 and A.23.1), the patterns suggest that SARS-CoV-2 has a great deal

230 of possibilities for further evolution, presumably enabling persistence and avoid immune responses.
231 This emphasises the importance of genomic variant surveillance for monitoring for further changes in
232 virus biology that may have implications for spread and disease severity. Vaccine producers should be
233 prepared to accommodate such spike changes in the next generation of vaccine updates. In addition
234 to the spike protein, additional regions of high variance were observed in the nsp3 across all
235 *Sarbecoviruses* (Figure 2) in close bat and pangolins (Figure 3).

236 The high variance regions flanked and partially overlapped the Macro domain, which is
237 frequently associated with ADP-deribosylase activity (Frick et al. 2020)(Lei et al. 2018). Variance
238 observed in the ORF8 changes across the set was due to frequent deletion of this ORF, suggesting
239 that the encoded protein may be dispensable for human infection. Similar loss of ORF8 was observed
240 with the original SARS-CoV (Chiu et al. 2005) (Tang et al. 2006) and has been observed in several
241 SARS-CoV-2 lineages as the virus adapted to humans (Su et al. 2020) (Gong et al. 2020) (Young et al.
242 2020). The ORF9 (N protein) variance observed across *Sarbecoviruses* and the changes in this protein
243 in VOC strains suggest an additional region that may be adapting to human replication. The regions of
244 variance identified here may indicate either functional changes in SARS-CoV-2 proteins or amino acid
245 positions that can be changed without impairing the necessary functions of the protein. The relatively
246 high mutation rate of SARS-CoV-2 combined with the unprecedented number of SARS-CoV-2
247 infections in the world is resulting in massive viral adaptation. Additional experiments are required to
248 distinguish true functional changes from neutral evolution.

249 Finally, the detailed spike analysis of Figure 4 revealed 88 15aa spike domains showing high
250 variation while only 27 (31%) have accumulated substitutions or deletions in the current epidemic in
251 VOCs and VOIs indicating a large potential for tolerating future change. It is highly likely that a large
252 number of new SARS-CoV-2 variants with changes in these regions will evolve, compatible with similar
253 levels of virus replication but tolerating significant antigenic change in the coming years, unless global
254 SARS-CoV-2 spread is severely curtailed.

255

256 **Acknowledgements**

257 We thank all global SARS-CoV-2 sequencing groups for their open and rapid sharing of sequence
258 data and GISAID for providing an effective platform for making these data available. This work was
259 supported by the Wellcome, DFID - Wellcome Epidemic Preparedness – Coronavirus (AFRICO19,
260 grant agreement number 220977/Z/20/Z) awarded to MC. DLR and MC receive funding from the MRC
261 (MC_UU_1201412), by the UK Medical Research Council (MRC/UKRI) and the UK Department for
262 International Development (DFID) under the MRC/DFID Concordat agreement (grant agreement
263 number NC_PC_19060).

264

265 **References**

266 Andersen KG, Rambaut A, Lipkin WI, Holmes EC, Garry RF. 2020. The proximal origin of SARS-CoV-2. *Nat. Med.*
267 [Internet]. Available from: <http://www.nature.com/articles/s41591-020-0820-9>

268 Boni MF, Lemey P, Jiang X, Lam TT-Y, Perry BW, Castoe TA, Rambaut A, Robertson DL. 2020. Evolutionary
269 origins of the SARS-CoV-2 sarbecovirus lineage responsible for the COVID-19 pandemic. *Nat.*
270 *Microbiol.* 5:1408–1417.

271 Chan YA, Zhan SH. 2020. Single source of pangolin CoVs with a near identical Spike RBD to SARS-CoV-2.
272 Genomics Available from: <http://biorxiv.org/lookup/doi/10.1101/2020.07.07.184374>

273 Chiu RWK, Chim SSC, Tong Y, Fung KSC, Chan PKS, Zhao G, Lo YMD. 2005. Tracing SARS-CoV-2 Variant
274 with Large Genomic Deletion. *Emerg. Infect. Dis.* 11:168–170.

275 Eddy SR. 1996. Hidden Markov models. *Curr. Opin. Struct. Biol.* 6:361–365.

276 Eddy SR. 1998. Profile hidden Markov models. *Bioinformatics* 14:755–763.

277 Eddy SR. 2011. Accelerated Profile HMM Searches. *PLOS Comput. Biol.* 7:e1002195.

278 Edgar RC. 2010. Search and clustering orders of magnitude faster than BLAST. *Bioinformatics* 26:2460–2461.

279 Frick DN, Virdi RS, Vuksanovic N, Dahal N, Silvaggi NR. 2020. Molecular Basis for ADP-Ribose Binding to the
280 Mac1 Domain of SARS-CoV-2 nsp3. *Biochemistry* 59:2608–2615.

281 Gong Y-N, Tsao K-C, Hsiao M-J, Huang C-G, Huang P-N, Huang P-W, Lee K-M, Liu Yi-Chun, Yang S-L, Kuo R-L, et
282 al. 2020. SARS-CoV-2 genomic surveillance in Taiwan revealed novel ORF8-deletion mutant and clade
283 possibly associated with infections in Middle East. *Emerg. Microbes Infect.* 9:1457–1466.

284 Henikoff S, Henikoff JG. 1992. Amino acid substitution matrices from protein blocks. *Proc. Natl. Acad. Sci. U. S.*
285 A. 89:10915–10919.

286 Hoffmann M, Kleine-Weber H, Pöhlmann S. 2020. A Multibasic Cleavage Site in the Spike Protein of SARS-CoV-
2 Is Essential for Infection of Human Lung Cells. *Mol. Cell* 78:779–784.e5.

288 Katoh K, Standley DM. 2013. MAFFT Multiple Sequence Alignment Software Version 7: Improvements in
289 Performance and Usability. *Mol. Biol. Evol.* 30:772–780.

290 Lam TT-Y, Jia N, Zhang Y-W, Shum MH-H, Jiang J-F, Zhu H-C, Tong Y-G, Shi Y-X, Ni X-B, Liao Y-S, et al. 2020.
291 Identifying SARS-CoV-2-related coronaviruses in Malayan pangolins. *Nature* 583:282–285.

292 Lei J, Kusov Y, Hilgenfeld R. 2018. Nsp3 of coronaviruses: Structures and functions of a large multi-domain
293 protein. *Antiviral Res.* 149:58–74.

294 Li Q, Guan X, Wu P, Wang X, Zhou L, Tong Y, Ren R, Leung KSM, Lau EHY, Wong JY, et al. 2020. Early
295 Transmission Dynamics in Wuhan, China, of Novel Coronavirus–Infected Pneumonia. *N. Engl. J.*
296 *Med.*:NEJMoa2001316.

297 Liu P, Chen W, Chen J-P. 2019. Viral Metagenomics Revealed Sendai Virus and Coronavirus Infection of
298 Malayan Pangolins (*Manis javanica*). *Viruses* 11:979.

299 MacLean OA, Lytras S, Weaver S, Singer JB, Boni MF, Lemey P, Kosakovsky Pond SL, Robertson DL. 2021.
300 Natural selection in the evolution of SARS-CoV-2 in bats created a generalist virus and highly capable
301 human pathogen. Tully D, editor. *PLOS Biol.* 19:e3001115.

302 Masembe C, Phan MVT, Robertson DL, Cotten M. 2020. Increased resolution of African Swine Fever Virus
303 genome patterns based on profile HMM protein domains. Genomics Available from:
304 <http://biorxiv.org/lookup/doi/10.1101/2020.01.12.903104>

305 Phan MVT, Ngo Tri T, Hong Anh P, Baker S, Kellam P, Cotten M. 2018. Identification and characterization of
306 Coronaviridae genomes from Vietnamese bats and rats based on conserved protein domains. *Virus*
307 *Evol.* [Internet] 4. Available from:
308 <https://academic.oup.com/ve/article/doi/10.1093/ve/vey035/5250438>

309 Su YCF, Anderson DE, Young BE, Linster M, Zhu F, Jayakumar J, Zhuang Y, Kalimuddin S, Low JGH, Tan CW, et al.
310 2020. Discovery and Genomic Characterization of a 382-Nucleotide Deletion in ORF7b and ORF8

311 during the Early Evolution of SARS-CoV-2. Schultz-Cherry S, editor. *mbio* 11:e01610-20,
312 /mbio/11/4/mbio.01610-20.atom.

313 Tang JW, Cheung JLK, Chu IMT, Sung JY, Peiris M, Chan PKS. 2006. The Large 386-nt Deletion in SARS-
314 Associated Coronavirus: Evidence for Quasispecies? *J. Infect. Dis.* 194:808-813.

315 Xiao K, Zhai J, Feng Y, Zhou N, Zhang X, Zou J-J, Li N, Guo Y, Li X, Shen X, et al. 2020. Isolation of SARS-CoV-2-
316 related coronavirus from Malayan pangolins. *Nature* 583:286–289.

317 Yang X, Yu Y, Xu J, Shu H, Xia J, Liu H, Wu Y, Zhang L, Yu Z, Fang M, et al. 2020. Clinical course and outcomes of
318 critically ill patients with SARS-CoV-2 pneumonia in Wuhan, China: a single-centered, retrospective,
319 observational study. *Lancet Respir. Med.*:S2213260020300795.

320 Young BE, Fong S-W, Chan Y-H, Mak T-M, Ang LW, Anderson DE, Lee CY-P, Amrun SN, Lee B, Goh YS, et al.
321 2020. Effects of a major deletion in the SARS-CoV-2 genome on the severity of infection and the
322 inflammatory response: an observational cohort study. *Lancet Lond Engl*. 396:603–611.

323 Zhang T, Wu Q, Zhang Z. 2020. Probable Pangolin Origin of SARS-CoV-2 Associated with the COVID-19
324 Outbreak. *Curr. Biol.*:S0960982220303602.

325 Zhou H, Chen X, Hu T, Li J, Song H, Liu Y, Wang P, Liu D, Yang J, Holmes EC, et al. 2020. A novel bat coronavirus
326 reveals natural insertions at the S1/S2 cleavage site of the Spike protein and a possible recombinant
327 origin of HCoV-19. *Microbiology* Available from:
328 <http://biorxiv.org/lookup/doi/10.1101/2020.03.02.974139>

329 Zhou P, Yang X-L, Wang X-G, Hu B, Zhang L, Zhang W, Si H-R, Zhu Y, Li B, Huang C-L, et al. 2020. A pneumonia
330 outbreak associated with a new coronavirus of probable bat origin. *Nature* 579:270–273.

331 Supplementary Material.

332

333 **Supplementary Table 1. Close bat coronaviruses.**

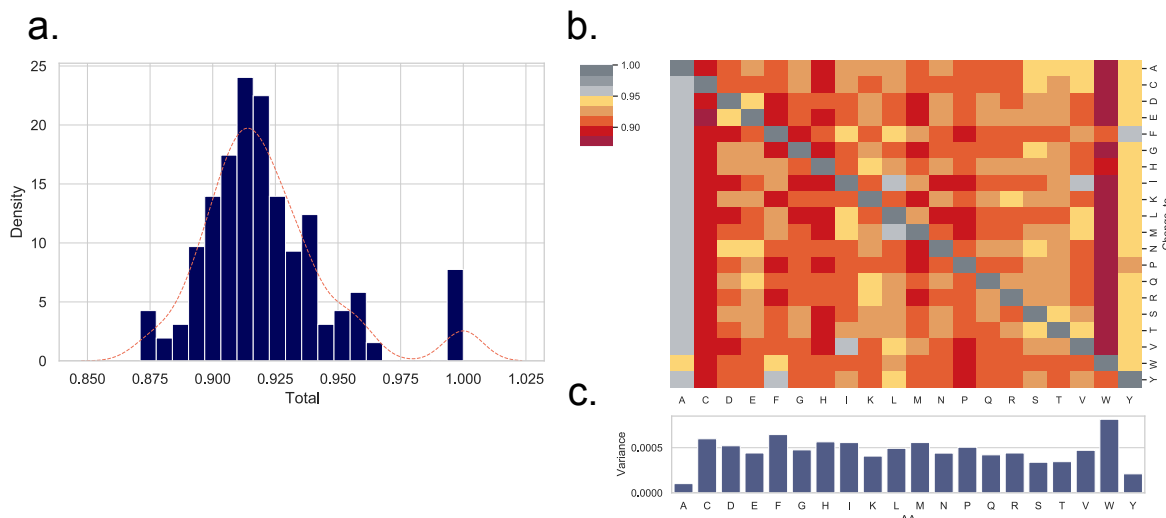
Genome name	GenBank or GISAID	Year	Reference
RpYN06	EPI_ISL_1699446	2020	unpublished
RmYN02	EPI_ISL_412977	2019	Zhou et al. <i>Curr Biol.</i> 2020 Jun 8;30(11):2196-2203.e3. PMID: 32416074
PrC31	EPI_ISL_1098866	2018	unpublished
RaTG13	MN996532	2013	Zhou et al. <i>Nature.</i> 2020 Mar;579(7798):270-273 PMID: 32015507
RshSTT182	EPI_ISL_852604	2010	http://biorxiv.org/lookup/doi/10.1101/2021.01.26.428212
RshSTT200	EPI_ISL_852605	2010	http://biorxiv.org/lookup/doi/10.1101/2021.01.26.428212
CoVZ45	MG772933	2017	Hu et al. <i>Emerg Microbes Infect</i> 7 (1), 154 (2018) PMID: 30209269
CoVZXC21	MG772934	2015	Hu et al. <i>Emerg Microbes Infect</i> 7 (1), 154 (2018) PMID: 30209269
RaCS203	MW251308	2020	Wacharapluesadee et al. <i>Nat Commun.</i> 2021 12(1):972 PMID: 33563978
Rc-0319	LC556375	2013	Murakami et al. <i>EID</i> 2020 Dec;26(12):3025-3029 PMID: 33219796
GX-P4L	MT040333	2017	Lam et al. 2020. <i>Nature</i> 583:282-285. PMID: 32218527
GX-P1E	MT040334	2017	Lam et al. 2020. <i>Nature</i> 583:282-285. PMID: 32218527
GX-P5L	MT040335	2017	Lam et al. 2020. <i>Nature</i> 583:282-285. PMID: 32218527
GX-P5E	MT040336	2017	Lam et al. 2020. <i>Nature</i> 583:282-285. PMID: 32218527
MP789	MT121216	2019	Liu et al. <i>PLoS Pathog.</i> 16 (5), e1008421 (2020) PMID: 32407364

334

335 Supplementary Figure 1 to illustrate pHMM detection of amino acid changes.

336 We sought to illustrate the ability of pHMMs to detect amino acid differences between a
337 reference and a query sequence. A reference peptide containing the twenty amino acids was used to
338 prepare a pHMM. A test set of mutant sequences was prepared by sequentially changing each amino
339 acid to each of the other 20 amino acids. This set of 400 sequences was then queried with the wildtype
340 20aa profile HMM, the bit-scores describing each match were collection. The distribution of bit-scores
341 from the 400 pHMM matches (Supplementary Figure 1a) was broad, consistent with the methods ability

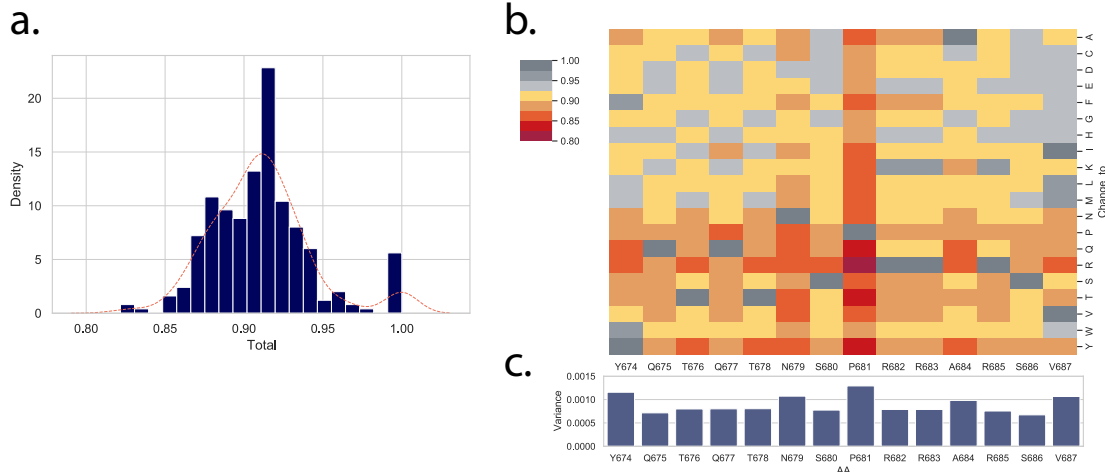
342 to report not only an amino acid changes but the type of amino acid change. The pattern of all amino
343 acid changes across all 20 AA peptide is displayed in clustermap (Supplementary Figure 1b) with each
344 column corresponding to a single amino acid and each row showing the score if that amino acid were
345 changed to another amino acid. An amino acid that is frequent (e.g. alanine (A)) shows higher bit-scores
346 across the set of changes than rarer amino acids such as cysteine (C), histidine (H), tryptophan (W) or
347 proline (P). This spectrum closely reflects the BLOSUM62 substitution matrix (Henikoff and Henikoff
348 1992) and demonstrates the capacity of a pHMM match both to detect changes in proteins as they
349 evolve and to distinguish different types of changes.



350
351 **Supplementary Figure 1.** pHMM bit-score values as a measure of the type of amino acid change. A
352 sequence encoding all 20 amino acids (ACDEFGHIKLMNPQRSTVWY) was used to prepare a pHMM.
353 A test set of mutant sequences was prepared by changing each amino acid to each of the other 20
354 amino acids. This set of 400 sequences was then queried with the wildtype 20aa profile HMM, bit-
355 scores for each match were collected in a matrix. **(a)** a histogram of all observed normalized bit-scores,
356 the peak at 1.00 is due to changes to self (e.g. A to A change). **(b)** heatmap of normalized bit-scores,
357 each columns represents a position in the 20 AA wt peptide, each row represents a change at that
358 position to the indicated amino acid. The normalized bit-scores were color coded with no change from
359 wildtype amino acid (dark grey) to the largest change from the wildtype amino acid (dark red). **(c)**
360 Variance of normalized bit-scores from panel b were calculated for each position.
361

362 In a second analysis we examined a peptide sequence spanning the important furin cleavage
363 site in the SARS-CoV-2 spike protein. Mutations in this region have appeared in several VOCs (A.23.1:
364 P681R, B.1.1.7: P681H, B.1.525: Q677H) and we wanted to document the sensitivity of pHMM
365 matching to detect single amino acid changes. Similar to Supplementary Figure 1, we prepared a pHMM
366 from the wildtype 14aa sequence spanning the furin site. For a test set we systematically change
367 position to each of the 20 amino acids and then gathered the bit-scores for the wildtype pHMM matching
368 each test peptide. Similar to Supplementary Figure 1, the range of normalized bit-scores scores
369 included a peak at 1.00 (self sequence matched to self) plus a range of lower values demonstrating
370 the breadth of possible pHMM bits-scores for any possible single amino acid changes in the 14 amino
371 acid peptide (Supplementary Figure 2a). The heatmap of the resulting normalized bit-scores
372 (Supplementary Figure 2b) reveals some patterns. Most changes of the proline adjacent to the

373 cleavage site resulted in a large reduction in bit-scores, whereas other changes resulted in detectable,
374 distinct, but less dramatic bit-scores.
375



376
377 **Supplementary Figure 2. Amino acid changes across the P681 region of the spike protein.** A 14
378 amino acid sequence spanning the SARS-CoV-2 spike position 681 and the adjacent furin cleavage
379 site (YQTQTNSPRRARSV) was used to prepare a pHMM. A test set of mutant sequences was
380 prepared by changing each amino acid to each of the other 20 amino acids. This set of 280 sequences
381 was then queried with the wildtype 14aa pHMM, bit-scores were collected. Panel a, a histogram of all
382 observed normalized bit-scores, the peak at 1.00 due to changes to self (e.g. A to A change). Panel b,
383 heatmap of normalized bit-scores, each columns represents a position in the 14 AA wt peptide, each
384 row represents a change at that position to the indicated amino acid. The normalized bit-scores were
385 color coded with no change from wildtype amino acid (dark grey) to the largest change from the wildtype
386 amino acid (dark red). Panel C. Variance of normalized bit-scores from Panel b were calculated for
387 each amino acid position across the peptide.